CCC Annual Report

UIUC, August 19, 2015

Pressure-energy Model of Tundish, Slide-gate and Nozzle Flow and Application to Avoiding Aspiration

Hyunjin Yang and Brian G. Thomas

Department of Mechanical Science & Engineering
University of Illinois at Urbana-Champaign

Motivation

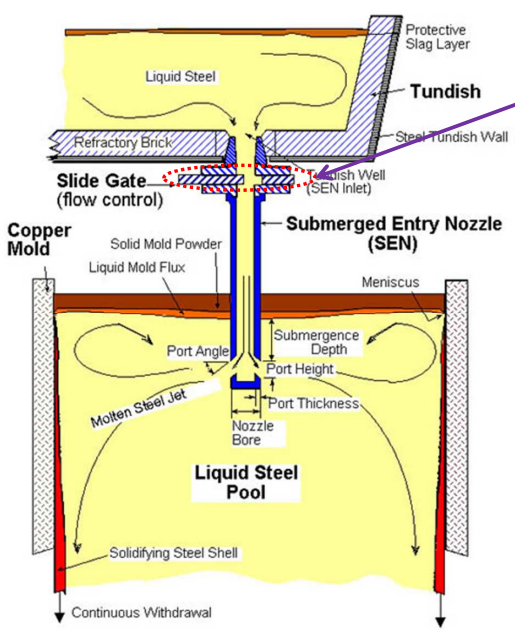

Fig 1. Schematic of continuous casting (Continuous Casting Consortium website)

Negative pressure from flow restriction — Control gravity-driven flow by slide-gate

Aspiration — $P_{inside} < P_{atm}$ Air sucked in through crack / joint …

Re-oxidation — Oxygen reacts with steel, eg. $Al + O_2 \rightarrow Al_2O_3$ (Alumina)

Attach to nozzle walls → **Clogging**

Captured in solidified shell → **Inclusion**

- Likely in re-circulation regions.
- Change the flow pattern.
- productivity loss

- Defect in the final product
- Causes lower strength and toughness

The problem

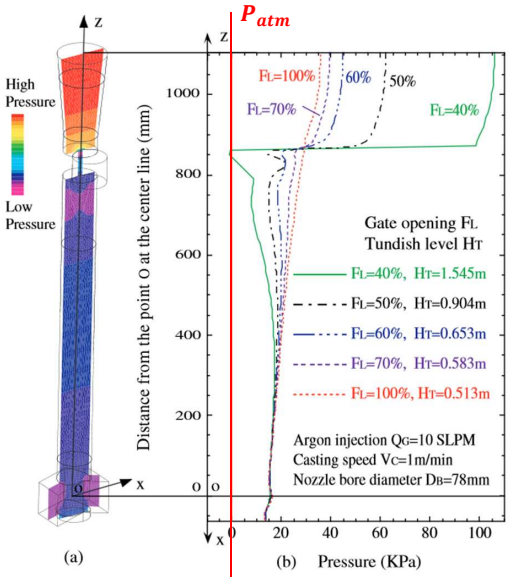

Fig 2. **Pressure distribution** in SEN with respect to slide-gate opening fractions (Bai and Thomas, 2001) **(hydrostatic pressure is not included in this figure)**

Fig 3. Cross-section of SEN nozzle with **clogging** (www.iehk.rwth-aachen.de)

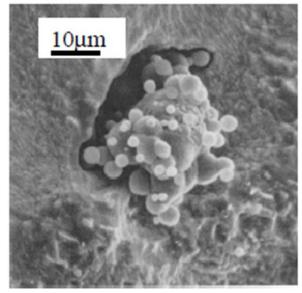

Fig 4. **Captured Alumina** cluster in the slab (Thomas, ME550 lecture note)

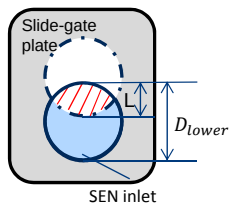

$$F_L = \frac{L}{D_{lower}}$$

Literature review: how to avoid aspiration?

1. **Make vacuum** or **Ar** atmosphere outside of slide-gate
   - Expensive Argon facility (Castrip/Nucor)
   - Expensive vacuum facility (POSCO, patent 2010, KR20120026720

2. **Inject** Argon gas into nozzle (Bai and Thomas, 2001)
   - Inject Ar gas through porous refractory
     -> increase the minimum pressure in SEN (1of ~5 mechanisms)
     -> Fills recirculation regions in SEN with argon
   - Flood the slide-gate gap with Argon gas
   - But Ar gas changes mold flow pattern, so could be harmful:

3. Suggest a **better SEN geometry** : current work
   - Casting speed, Ar gas flow rate, slide-gate opening, tundish level and nozzle geometry are **inter-related**.
   - Develop analytical model for pressure distribution in flow system
   - Optimize SEN design to minimize air aspiration

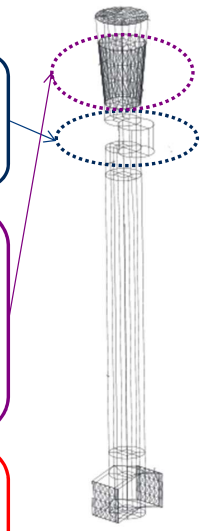

Fig 5. SEN geometry (Bai and Thomas, 2001)

Objectives

1. Develop **simple model to estimate pressure distribution in nozzle flow system:**

   - Use analytical approach:
     -> **1D pressure-energy equation** with **energy losses**
     -> **calculate pressure distribution** from Tundish top surface to Mold top surface

   - Compare with 3D turbulent two-phase computational model:
     -> $k - \epsilon$ model with wall functions for a rough wall
     -> Eulerian-Eulerian two phase model

2. **Propose** a new **nozzle design** to **avoid** air aspiration.

   - **Parametric studies** with analytical model
   - Propose **new SEN diameter**

Part 1.

1D Pressure-energy Model Development

1D model of pressure Distribution of flow system (from mold to tundish)

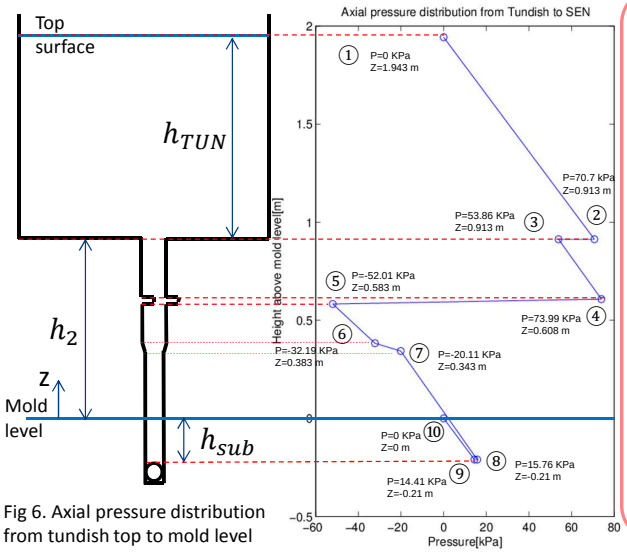

Fig 6. Axial pressure distribution from tundish top to mold level

⑩ $P_{10} = 0$

⑨ $P_9 = P_{10} + \rho g z_{109}$

Assumes that the flow velocity is dissipated on the top surface (at ⑨)

⑧ $P_8 = P_9 - \frac{1}{2}\rho V_{SEN}^2 + \frac{1}{2}\rho V_{port}^2 + \rho e_{Lport} + \rho e_{Lelbow}$

⑦ $P_7 = P_8 - \rho g z_{78} + \frac{1}{2}\rho V_{SEN}{}^2 f \frac{z_{78}}{D_{SEN,L}}$

⑥ $P_6 = P_7 - \rho g z_{67} + \frac{1}{2}\rho V_{SEN}^2 - \frac{1}{2}\rho V_{GAP}^2 \boldsymbol{\chi}^2 + \frac{1}{2}\rho V_{lower}{}^2 f \frac{z_{67}}{D_{lower}} + \rho e_{Lcont}$

⑤ $P_5 = P_6 - \rho g z_{56} + \frac{1}{2}\rho V_{GAP}{}^2 \boldsymbol{\chi}^2 - \frac{1}{2}\rho V_{GAP}^2 \boldsymbol{\gamma}^2 + \frac{1}{2}\rho V_{lower}{}^2 f \frac{z_{56}}{D_{lower}}$

④ $P_4 = P_5 - \rho g z_{45} - \frac{1}{2}\rho V_{UTN}{}^2 + \frac{1}{2}\rho V_{GAP}^2 \boldsymbol{\gamma}^2 + \frac{1}{2}\rho V_{UTN}{}^2 f \frac{z_{45}}{D_{Slide}} + \rho e_{Lslide} \boldsymbol{\zeta}$

③ $P_3 = P_4 - \rho g z_{34} + \frac{1}{2}\rho V_{UTN}^2 f \frac{z_{34}}{D_{UTN}}$

② $P_2 = P_3 + \frac{1}{2}\rho V_{UTN}^2 + \rho e_{Ltun} + \Delta P_{two}$

① $P_1 = P_2 - \rho g z_{12}$

P_x : gage pressure at the point x
ρ : liquid steel density
V_{SEN} : velocity in SEN lower part
V_{port} : velocity in port
V_{UTN} : velocity in UTN
V_{GAP} : velocity in slide-gate opening
V_{lower} : velocity in lower nozzle

$z_{ab} = z_a - z_b$
f : friction factor
g : gravity acceleration
$D_{SEN,L}$: lower part SEN diameter
D_{UTN} : UTN diameter
D_{Slide} : slide-gate diameter
D_{lower} : lower nozzle diameter

ρe_{Lport} : pressure loss across port (from velocity drop & friction) = 0
ρe_{Lelbow} : pressure loss across the port (from direction change)
ρe_{Lcont} : pressure loss across tapered region
ρe_{Lslide} : pressure loss across the slide-gate
ρe_{Ltun}: pressure loss across tundish bottom to UTN
ΔP_{two} : pressure drop by buoyancy (small but included)

$\boldsymbol{\beta}, \boldsymbol{\gamma}, \boldsymbol{\chi}$: velocity drop constants

$\boldsymbol{\zeta}$: slide-gate pressure loss constant

1D model of pressure Distribution: Losses in the model

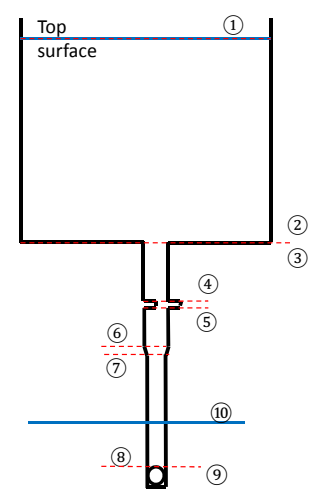

Fig 7. Schematic from tundish to port

Pressure loss components

- At ② ~ ③

$$\rho e_{Ltun} = \frac{1}{2}\rho V_{SEN}{}^2 \left(\frac{2A_{SEN,L}}{A_{TUN}}\right)^2 \left(\frac{A_{TUN}}{2A_{UTN}} - 1\right)^2 \qquad \Delta P_{two} = \frac{\rho g V_{gas}}{A_{UTN}}$$

- At ④~⑤

$$\rho e_{Lslide} = \frac{1}{2}\rho V_{UTN}{}^2 \left\{\left(\frac{1}{\mu} - 1\right)^2 \left(\frac{A_{SEN,L}}{A_{GAP}}\right)^2 + \left(\frac{A_{SG}}{A_{GAP}} - \frac{A_{GAP}}{A_{SG}}\right)^2 \left(\frac{A_{SEN,L}}{A_{SG}}\right)^2\right\}$$

Liu and Thomas (2012)

- At ⑥~⑦

$$\rho e_{Lcont} = \frac{1}{2}\rho V_{SEN}{}^2 \left(\frac{A_{UTN}}{A_{SEN,L}} - 1\right)^2$$

- At ⑧~⑨

$$\rho e_{Lport} = \frac{1}{2}\rho V_{SEN}{}^2 \left(\frac{A_{SEN,L}}{2A_{port}} - 1\right)^2 \qquad \rho e_{Lelbow} = K\frac{1}{2}\rho V_{SEN}{}^2$$

- "Pipe" friction loss in the system

$$\sum \rho e_{Lf} = \frac{1}{2}\rho V_{UTN}{}^2 f \frac{x_{27}}{D_{UTN}} + \frac{1}{2}\rho V_{SEN}{}^2 f \frac{x_{78}}{D_{SEN,L}}$$

$$V_{UTN} = \frac{Q}{A_{UTN}(1-\alpha)} \qquad V_{lower} = \frac{Q}{A_{lower}(1-\alpha)}$$

$$V_{SEN} = \frac{Q}{A_{SEN,L}(1-\alpha)} \qquad V_{GAP} = \frac{Q}{A_{GAP}(1-\alpha)}$$

$$V_{port} = \frac{Q}{A_{SEN}(1-\alpha) \times \boldsymbol{\beta}}$$

$A_{SEN,L}$: cross-section area of lower part SEN
A_{TUN} : cross-section area of tundish bottom
A_{UTN} : cross-section area of UTN
A_{GAP} : cross-section area of slide-gate opening
A_{SG} : cross-section area of fully opened slide-gate
K : minor loss coefficient of the elbow-shaped port
-> 0.2 is used for the 60x80 mm 75^0 port [White, 2011]
Q : liquid steel flow rate = casting speed V_c × Mold cross-section area wt

A_{lower} : cross-section area of lower nozzle

$$\mu = 0.63 + 0.37\left(\frac{A_{GAP}}{A_{SG}}\right)^3$$

Liu and Thomas (2012)

Determination of Model constant γ

1. Gamma γ at the point ⑤ (ref.: Armaly et al.,1983)

- In the sudden expanded pipe turbulent flow (backward-facing step flow), the **recirculation zone size x_1** is independent of the Re, but a function of geometry.
- 2D approximation is available for Re<400 and Re>6600 (belong to the latter for this case).
- Expansion rate ER $= \frac{inlet\ height}{outle\ height} = \frac{1}{f_L}$ (since $A_{UTN} = A_{slide}$)

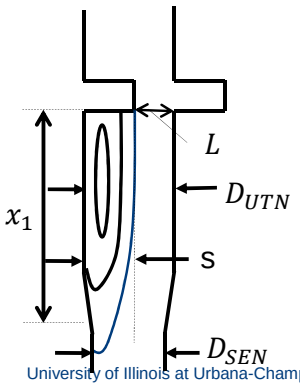

- According to the previous experiment study (Armaly et al., 1983):

ER=2 : $\frac{x_1}{s} \cong 8$
ER=1.2 : $\frac{x_1}{s} \cong 6$
ER=1.1 : $\frac{x_1}{s} \cong 5.5$

Let's call this Turbulence constant C_t

Determination of Model constant γ

- In case of Case 12, $f_L = 0.381$:
  - ER= $\frac{1}{f_L} = 2.62$
  - Through the Least Square Method with the Armaly experiment data, $C_t = 2.671223 \times ER + 2.671223$
  - $C_t = 9.67$ when ER=2.62
  - $x_1 = s \times C_t = 0.48\ m$
- S calculation: S=D_{lower}-L=D_{lower} (1-f_L)
- Assume, recirculation zone thickness h
  - Drops from S at ⑤ (plate bottom) to 0 at x_1
- Assume downward flow extends from center of recirculation zone (0.5S) to outer wall of D_{lower} :
- Define γ

$\gamma = \frac{L}{D_{lower} - 0.5S}$ -> average velocity at ⑤ = γV_{GAP}

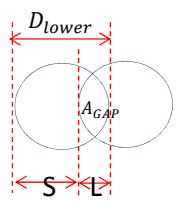

$$V_{GAP} = \frac{Q}{A_{GAP}(1-\alpha)}$$

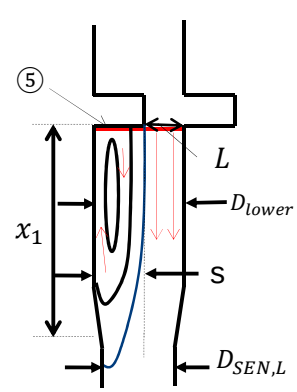

Determination of Model constant χ

2. Define Chi χ at point ⑥ (ref.: Armaly et al.,1983)

- Similar to γ, calculate average velocity at ⑥
- Using linear approximation for recirculation zone thickness.

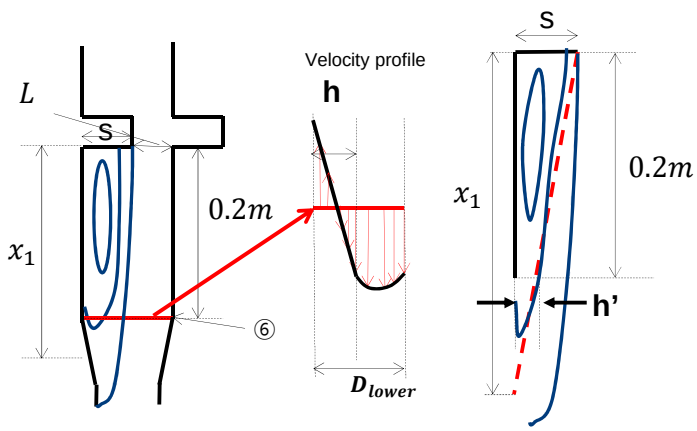

⇨ From similar triangles:

$$\therefore \mathbf{h'} = \frac{(x_1 - 0.2)\boldsymbol{s}}{x_1}$$

- $\chi = \frac{\boldsymbol{L}}{\boldsymbol{D_{lower} - 0.5h'}}$

: average velocity at ⑥ = $\chi\, V_{GAP}$

Determination of Model constants ζ&β

3. Zeta ζ

- The original Liu's model shows ~5% slide-gate opening f_L difference to the plant data in the non-clogged conditions, and ~10% difference in the clogged conditions.
- By increasing the pressure drop by the slide-gate ρe_{Lslide} with zeta $\boldsymbol{\zeta = 1.2}$, it matches better to the plant data on slide 19.

4. Beta β

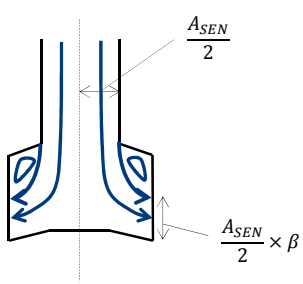

- Intuitively, $\boldsymbol{\beta}$ should be in the range of
  $1 \le \boldsymbol{\beta} \le \frac{A_{port}}{\frac{A_{SEN,L}}{2}} = 2.173$ (when $D_{SEN,L} = 75mm$)
- Since the port length is smaller than the port diameter, velocity drop is negligible:
  -> $\boldsymbol{\beta} = 1$ is chosen.

To check 1D model works properly

- At the P_1 in the bottom-up approach, the pressure is calculated by

$$P_1 = P_{atm} - \rho g(h_{TUN} + h_2) + \frac{1}{2}\rho V_{port}^2 + \Sigma \rho e_L$$

- We know $P_1 = P_{atm} = 0\ Pa\ (gage)$
- So, the model is validated by checking:
  - $P_1 = 0\ Pa \quad or$
  - $\underbrace{\rho g(h_{TUN} + h_2)}_{\text{Potential E (input)}} = \underbrace{\frac{1}{2}\rho V_{port}^2}_{\text{Kinetic E (output)}} + \underbrace{\rho e_{Ltun} + \Delta P_{two} + \rho e_{Lf} + \rho e_{Lslide} + \rho e_{Lcont} + \rho e_{Lport} + \rho e_{Ltee}}_{\Sigma \rho e_L \text{ : energy losses in the system}}$

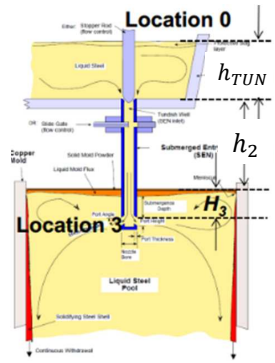

Fig 10. Height definition in continuous casting system (Liu and Thomas, 2012)

Geometry of the Baosteel UTN, Slidegate and SEN

- Geometry (from Baosteel)

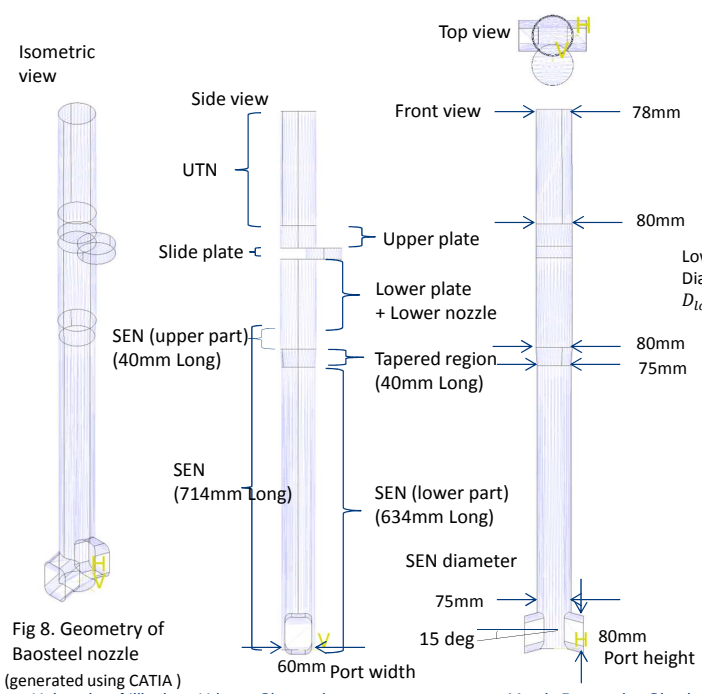

Fig 8. Geometry of Baosteel nozzle (generated using CATIA)

1. Relation between the A_{GAP} and f_A

$$f_A = \frac{A_{GAP}}{A_{SG}} \longrightarrow A_{GAP} = f_A A_{SG}$$

2. Relation between the f_A and f_L

$$f_A = \frac{2}{\pi}cos^{-1}(1 - f_L) - \frac{2}{\pi}(1 - f_L)\sqrt{1 - (1 - f_L)^2}$$

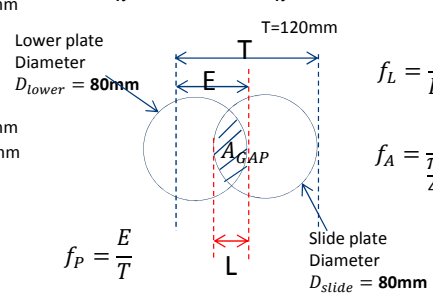

$$f_L = \frac{L}{D_{lower}}$$

$$f_A = \frac{A_{GAP}}{\frac{\pi}{4}D_{lower}^2}$$

$$f_P = \frac{E}{T}$$

3. Relation between the f_P and f_L

$$f_P = (1 - M)f_L + M \qquad M = \frac{T - D_{slide}}{T}$$

Geometry of the Baosteel UTN, Slidegate and SEN

- Original geometry of Baosteel

Geometry	Values
UTN bore diameter D_{UTN} (upper & lower)	78 mm & 80 mm
UTN length	255 mm
Upper plate thickness	50 mm
Upper plate bore diameter D_{upper}	80 mm
Slide plate thickness	25 mm
Slide plate bore diameter D_{slide}	80 mm
Lower plate + Lower nozzle bore diameter D_{lower}	80 mm
Lower plate + Lower nozzle Length	160 mm
SEN whole length	714 mm

Geometry	Values
SEN upper part bore diameter $D_{SEN,U}$	80 mm
SEN upper part length	40 mm
SEN tapered part length	40 mm
SEN lower part bore diameter $D_{SEN,L}$	75 mm
SEN lower part length	634 mm
Port angle	15 deg
Port width × height	60 mm × 80 mm
Port thickness	23.5 mm
Slab geometry	0.3×1.9 m

- In the 1D analytical model, UTN upper bore diameter is assumed to 80 mm.

Wall roughness consideration (for rough pipe)

1. From the real measurement on the SEN: ε (absolute roughness) $= 1.0\ mm$
   By the relation ε (absolute roughness) = k_s (physical roughness height)
   -> get $k_s = 1.0\ mm$ in SEN (wall function input for the computational model)
2. Calculate the relative roughness: $\frac{\varepsilon}{D_{SEN,L}} = \frac{1.0}{75} \cong 0.0133$, $\frac{\varepsilon}{D_{UTN}} = \frac{1.0}{80} \cong 0.0125$
3. From the Moody diagram, get $f_{SEN,L} = 0.042, f_{UTN} = 0.041$

$f_{SEN,L} = 0.042$

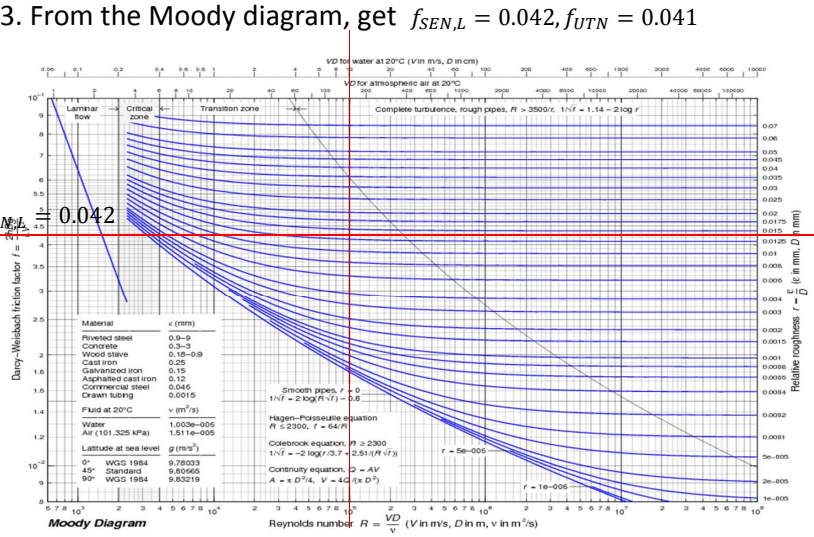

$\frac{\varepsilon}{D_{SEN,L}} \cong 0.0133$

Fig 9. Moody diagram (Moody, 1944)

Flow rate model to determine the slide-gate opening

1. Relation between the flow rate Q_{SEN} and the slide-gate opening f_A (Modified version based on Liu and Thomas (2012))

$$Q_{SEN} = A_{eff}\sqrt{\frac{2(h_{TUN}+H_2)g}{\left(\frac{2A_{SEN,L}}{A_{TUN}}\right)^2\left(\frac{A_{TUN}}{2A_{UTN}}-1\right)^2+\left(\frac{A_{SEN,L}}{2A_{port}}\right)^2+\left(\frac{A_{SEN,L}}{2A_{port}}-1\right)^2+\left(\frac{A_{SEN,L}}{A_{UTN}}\right)^2\left(\frac{A_{UTN}}{A_{SEN,L}}-1\right)^2+\left(\frac{A_{SEN,L}}{A_{UTN}}\right)^2 f\frac{L_{UTN}}{D_{UTN}}+f\frac{L_{SEN}}{D_{SEN}}+\left(\left(\frac{1}{\mu}-1\right)^2\left(\frac{A_{UTN}}{A_{GAP}}\right)^2+\left(\frac{A_{SG}}{A_{GAP}}-\frac{A_{GAP}}{A_{SG}}\right)^2\left(\frac{A_{UTN}}{A_{SG}}\right)^2\right)\zeta+K+B+C}}$$

2. Effective area calculation (two phase flow effect)

$$A_{eff} = \frac{V_c wt}{Q_{gas,h}+V_c wt}A = \frac{Q}{Q_{gas,h}+Q}A = (1-\alpha)A$$

Arbitrary cross-section area

3. μ calculation

$$\mu = 0.63 + 0.37\left(\frac{A_{GAP}}{A_{SG}}\right)^3 = 0.63 + 0.37 f_A^{\,3}$$

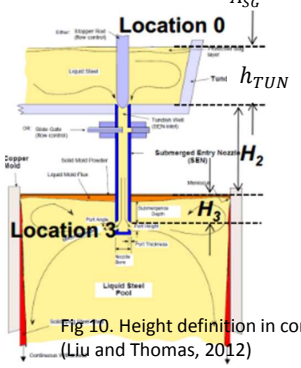

Fig 10. Height definition in continuous casting system (Liu and Thomas, 2012)

4. Gas volume fraction calculation (Thomas et al., 1994)

$$H_f = \frac{P_{atm}}{P_{port}} \times \frac{T_h}{T_\infty}$$

$$Q_{gas,h} = Q_{gas,SLPM} \times H_f \times 0.001/60 \quad [m^3/s]$$

$$\alpha = \frac{Q_{gas,h}}{Q_{gas,h}+V_c wt}$$

From Bai et al.(2001), for STP condition
P_{atm}=101325 Pa
T_∞=25°C

Q : liquid steel flow rate through SEN
$A_{SEN,L}$: lower part SEN cross-section area
A_{port} : area of one port outlet
A_{SG} : area of slide-gate when it is fully opened
A_{GAP} : area of opened slide-gate
α : gas volume fraction
L_{SEN} : SEN length
V_c : casting speed
w,t : caster width and thickness
$Q_{gas,h}$: gas flow rate when heat up
$Q_{gas,SLPM}$: gas flow rate with SLPM condition
K : minor loss coefficient of port
P_{port} : pressure at port outlet
g : gravity acceleration
f : friction factor
$\mu = 0.63 + 0.37\left(\frac{A_{GAP}}{A_{SG}}\right)^3$
f_A : slide-gate opening fraction
Q_{gas} : argon gas flow rate
D_{SEN} : diameter of the SEN
P_{atm} : atmosphere pressure
h_{sub} : submergence depth
T_h : gas temperature when heat up
T_∞ : room temperature
B : pressure drop by the buoyancy
C : clogging constant

Part 2.

Validation: Plant vs 1D model vs Fluent

Gate opening comparison: Plant measurement vs Flow rate model

No.	Grade	5ST/ 6ST	Slab geometry [m]	Casting speed V_C [m/min]	Argon flow rate Q_{gas}[SLPM]	tundish depth h_{TUN}[m]	slide-gate opening, F_L [%] Exp. data	slide-gate opening, F_L [%] Modified flow rate model
1	GL4G71R1	5ST	0.3×1.7	0.74	6.5	1.02	49	41.0
2	GL4G71R1	6ST	0.3×2.1	0.70	10.2	1.02	66	47.1
3	GL4G71R1	5ST	0.3×1.7	0.80	7	1.02	45	43.3
4	GL4G71R1	6ST	0.3×2.1	0.70	8.6	1.02	61	46.3
5	GL4G71R1	5ST	0.3×1.7	0.80	7	0.98	39	43.6
6	GL4G71R1	6ST	0.3×2.1	0.70	8.4	0.93	63	47.1
7	JV7Q13P6	5ST	0.3×2.1	0.70	4.2	1.02	37	44.2
8	JV7Q13P6	6ST	0.3×2.1	0.66	8.2	1.02	45	44.4
9	JV8Q13P6	5ST	0.3×2.1	0.66	4	1.10	46	41.7
10	JV8Q13P6	6ST	0.3×2.1	0.66	4.3	1.08	43	42.0
11	JU5P5CP6	5ST	0.3×1.9	0.60	6	1.03	40	38.1
12	JU5P5CP6	6ST	0.3×1.9	0.60	6	1.03	40	38.1

Data from Baosteel (Ruan, 2015)

- $\beta = 1, \zeta = 1.2, C = 0$ (clogging constant) are used for the modified flow rate model.
- Case 12 is chosen for the analysis.

- non-clogged
- clogged
- clogged severely

(according to the Baosteel data)

Operating condition

- Operating condition & Material property of case 12

Operating condition	Values
Slide-gate orientation	90 deg
Slide-gate opening f_L	0.4
Tundish depth h_{TUN}	1030 mm
Casting speed V_C	0.60 m/min
Argon gas flow rate Q_{argon}	6 SLPM
Submergence depth h_{sub}	0.21 m
Absolute roughness of the nozzle wall (ε)	1mm (Non-clogged condition)
Hot argon gas temperature T_h	1823 K
Hot argon gas pressure P_h	70.7 kPa (=$\rho_s g h_{TUN}$)

Material property	Values
Liquid steel density ρ_s	7000 kg/s
Liquid steel viscosity μ_s	0.006 Pas
Argon gas density ρ_g	1.6228 kg/s
Argon gas viscosity μ_g	2.125× 10^{-5} Pas

Gate opening comparison: Plant measurement vs Flow rate model

JU5P5CP6 6ST case 12 condition

Plant data: $f_L = 0.40$, $H_{TUN} = 1030\text{mm}$, $Q = 0.0057 m^3/s$

Flow rate model:

$Q = 0.0057 m^3/s$

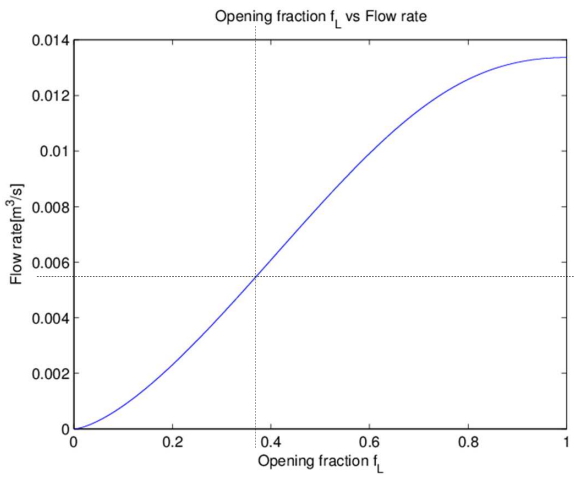

$f_L = 0.381$
$H_{TUN} = 1030\text{mm}$,

Fig 11. Relations between the slide-gate opening fraction f_L and the flow rate Q

1D Theoretical Pressure distribution: Case 12 condition (Bottom to Top)

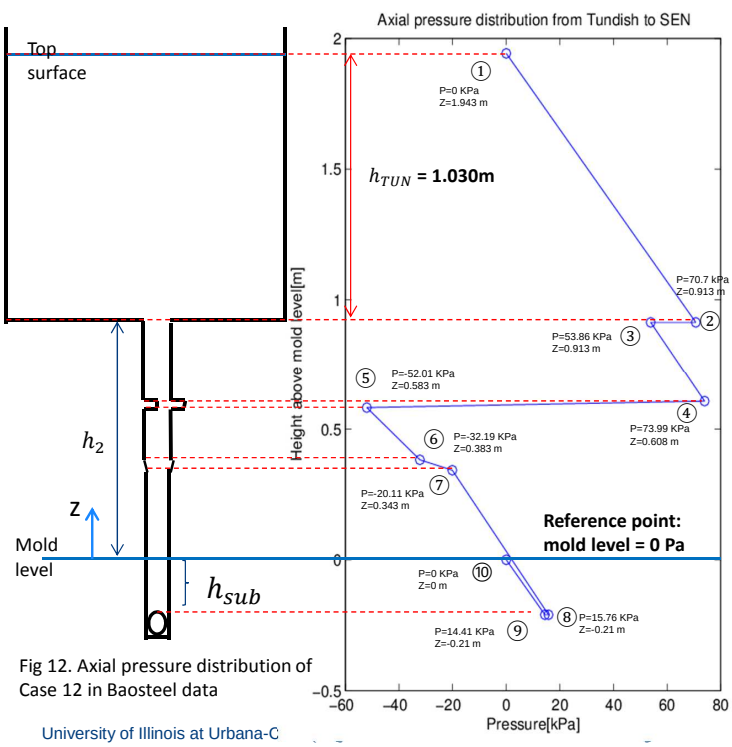

Fig 12. Axial pressure distribution of Case 12 in Baosteel data

- P_1 should be 0 Pa -> satisfied!
- At ②~③

  $\rho e_{Ltun} = 5.20\ kPa$
  $\Delta P_{Ltwo} = 6.42\ kPa$
- At ④~⑤

  $\rho e_{Lslide} \times \zeta = 91.62\ kPa \times 1.2 = 109.9\ kPa$
- At ⑥~⑦

  $\rho e_{Lcont} = 98.8\ Pa$
- At ⑧~⑨

  $\rho e_{Ltee} = 1.35\ kPa$
  $\rho e_{Lport} = 0\ Pa$
- Total friction loss

  $\sum \rho e_{Lf} = 3.61\ kPa$
- Model constants

  $\beta = 1.0 \quad \chi = 0.4609$
  $\gamma = 0.5465 \quad \zeta = 1.2$

Plant measurement vs Simulation: **Simulation of Case 12 condition**

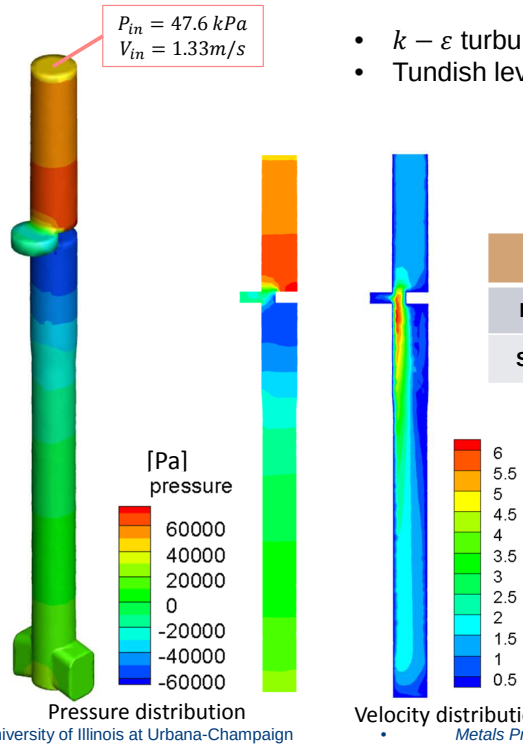

- $k - \varepsilon$ turbulence model + Eulerian Eulerian two phase model
- Tundish level calculation:

$$H_{TUN} = \frac{P_{in} + \frac{1}{2}\rho V_{in}^2 + \rho e_{Ltun} + \Delta P_{two}}{\rho g} = 0.984m$$

	Slide-gate opening f_L	Tundish level H_{TUN}	Flow rate Q
Plant data	**0.40**	**1030 mm**	**0.0057 m^3/s**
Simulation	**0.40**	**984 mm**	**0.0057 m^3/s**

Fig 13. Velocity and pressure distribution in nozzle by computational model

Analytical model vs simulation **Case 12 condition**

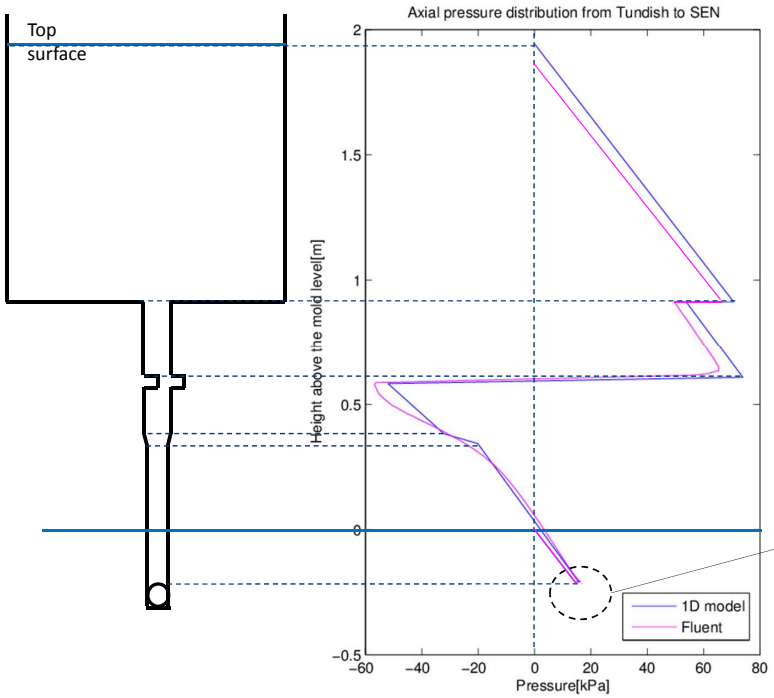

- The blue line is the 1D pressure model calculation result shown on slide 21 (the formula is on slide 7).
- The pink line is from the Fluent simulation result shown on slide 22, which has tundish level 984mm.

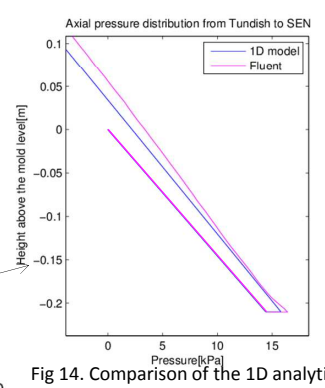

Fig 14. Comparison of the 1D analytical model and the Fluent pressure distribution

Part 3.

Parametric study: Change of casting conditions

Geometry of parametric study 1

- Parametric study 1 geometry

Geometry	Values
UTN bore diameter D_{UTN}	80 mm
UTN length	255 mm
Upper plate thickness	50 mm
Upper plate bore diameter D_{upper}	80 mm
Slide plate thickness	25 mm
Slide plate bore diameter D_{slide}	80 mm
Lower plate + Lower nozzle bore diameter D_{lower}	80 mm
Lower plate + Lower nozzle Length	160 mm

Geometry	Values
SEN upper part bore diameter $D_{SEN,U}$	80 mm
SEN upper part length	40 mm
SEN tapered part length	40 mm
SEN lower part bore diameter $D_{SEN,L}$	**75 mm (original) 52 mm ~ 100 mm (parametric study)**
SEN lower part length	714 mm
Port angle	15 deg
Port width × height	60 mm × 80 mm
Port thickness	23.5 mm
Slab geometry	0.3×1.9 m

- In the 1D analytical model, UTN upper bore diameter is assumed to 80 mm.
- Only $\boldsymbol{D_{SEN,L}}$ is changed from the original geometry

Operating condition of parametric study 1

- Operating condition & Material property of parametric study 1

Operating condition	Values
Slide-gate orientation	90 deg
Slide-gate opening f_L	**0.4 (original) 0.376~0.454 (parametric study)**
Tundish depth h_{TUN}	1030 mm
Casting speed V_C	0.60 m/min
Argon gas flow rate Q_{argon}	6 SLPM
Submergence depth h_{sub}	0.21 m
Absolute roughness of the nozzle wall (ε)	1mm (Non-clogged condition)
Hot argon gas temperature T_h	1823 K
Hot argon gas pressure P_h	70.7 kPa (=$\rho_s g h_{TUN}$)

Material property	Values
Liquid steel density ρ_s	7000 kg/s
Liquid steel viscosity μ_s	0.006 Pas
Argon gas density ρ_g	1.6228 kg/s
Argon gas viscosity μ_g	2.125× 10^{-5} Pas

- Same to the original operating condition except slide-gate opening f_L depending on the SEN lower part diameter $D_{SEN,L}$

Parametric study 1: SEN diameter $D_{SEN,L}$ (fixed all other diameters)

Vary SEN lower part diameter $D_{SEN,L}$, also vary slide-gate opening f_L,

(to maintain flow rate $Q = 0.0057 m^3/s$, keeping all other diameters to $80mm$)

$D_{SEN,L} = 52mm$

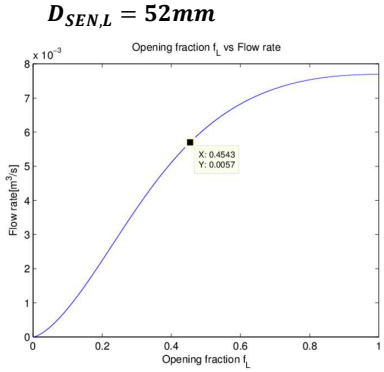

$D_{SEN,L} = 58mm$

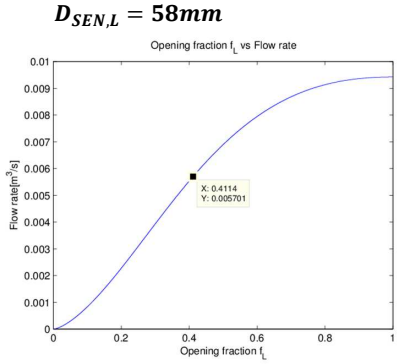

$D_{SEN,L} = 100\ mm$

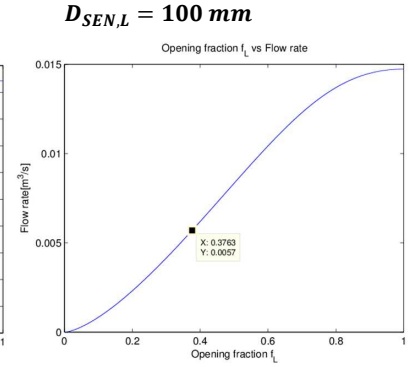

Cases	$D_{SEN,L}$ [mm]	f_{SEN} *(friction factor)*	f_L , L [mm]	f_A , A [mm^2]	**Flow rate** Q [m^3/s]
Original condition	75	0.042	0.381, [30.48] (from slide 19)	0.266, [1337]	0.0057
Run 1	52	0.048	0.454, [36.32]	0.341, [1716]	0.0057
Run 2	58	0.047	0.411, [32.88]	0.296, [1488]	0.0057
Run 3	100	0.038	0.376, [30.08]	0.261, [1312]	0.0057

(All other casting conditions are same to the previous slide table)

Fig 15. Relations between the slide-gate opening fraction f_L and the flow rate Q depending on the SEN diameter

Parametric study 1 results: SEN diameter $D_{SEN,L}$ (fixed all other diameters)

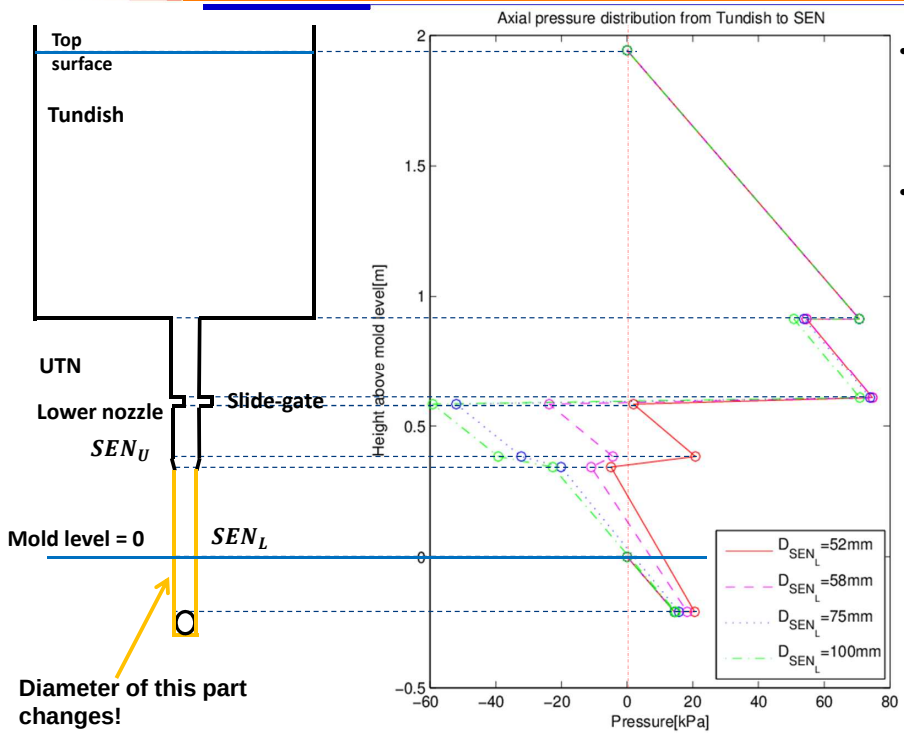

- Varying only lower part SEN diameter (and gate opening fraction to keep flow rate constant)
- Negative pressure is avoided at slide-gate for $D_{SEN,D}$< 52mm

Fig 16. Axial pressure distributions for different SEN diameters

Geometry of the parametric study 2

Geometry	Values
UTN bore diameter D_{UTN}	**80 mm (original) 49.1 mm ~ 100 mm (parametric)**
UTN length	255 mm
Upper plate thickness	50 mm
Upper plate bore diameter D_{upper}	**80 mm (original) 49.1 mm ~ 100 mm (parametric)**
Slide plate thickness	25 mm
Slide plate bore diameter D_{slide}	**80 mm (original) 49.1 mm ~ 100 mm (parametric)**
Lower plate + Lower nozzle bore diameter D_{lower}	**80 mm (original) 49.1 mm ~ 100 mm (parametric)**
Lower plate + Lower nozzle Length	160 mm

Geometry	Values
SEN upper part bore diameter $D_{SEN,U}$	**80 mm (original) 49.1 mm ~ 100 mm (parametric)**
SEN upper part length	40 mm
SEN tapered part length	40 mm
SEN lower part bore diameter $D_{SEN,L}$	**75 mm (original) 52 mm ~ 100 mm (parametric study)**
SEN lower part length	714 mm
Port angle	15 deg
Port width × height	60 mm × 80 mm
Port thickness	23.5 mm
Slab geometry	0.3×1.9 m

Operating condition of parametric study 2

Operating condition	Values
Slide-gate orientation	90 deg
Slide-gate opening f_L	**0.4 (original) 0.278~1.000 (parametric study)**
Tundish depth h_{TUN}	1030 mm
Casting speed V_C	0.60 m/min
Argon gas flow rate Q_{argon}	6 SLPM
Submergence depth h_{sub}	0.21 m
Absolute roughness of the nozzle wall (ε)	1mm (Non-clogged condition)
Hot argon gas temperature T_h	1823 K
Hot argon gas pressure P_h	70.7 kPa (=$\rho_s g h_{TUN}$)

Material property	Values
Liquid steel density ρ_s	7000 kg/s
Liquid steel viscosity μ_s	0.006 Pas
Argon gas density ρ_g	1.6228 kg/s
Argon gas viscosity μ_g	2.125× 10^{-5} Pas

- Same to the original operating condition except slide-gate opening f_L depending on the SEN lower part diameter $D_{SEN,L}$

Parametric study 2: All nozzle diameter ($D_{UTN} = D_{upper} = D_{slide} = D_{lower} = D_{SEN,U} = D_{SEN,L}$)

Vary lower SEN diameter $D_{SEN,L}$ (but also vary 5 other nozzle diameters to keep all 4 diameters the same).
Also vary slide-gate opening f_L, (to maintain constant flow rate $Q = 0.0057 m^3/s$)

$D_{SEN,L} = 49.1\ mm$ $D_{SEN,L} = 58\ mm$ $D_{SEN,L} = 75\ mm$ $D_{SEN,L} = 100\ mm$

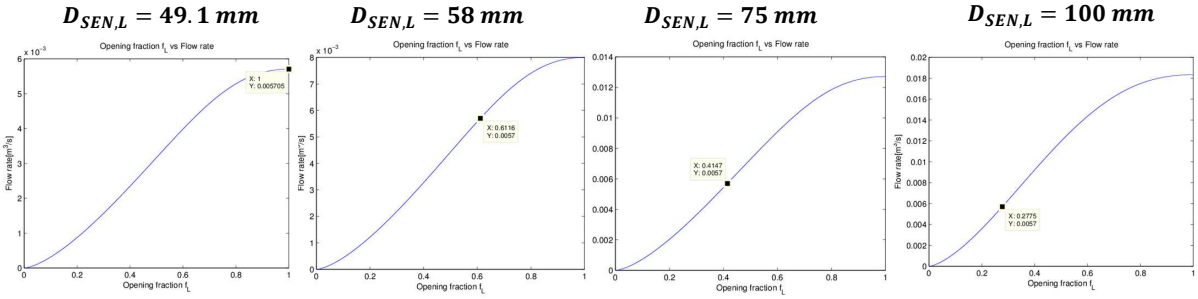

Note: remove taper part of SEN

Cases	$D_{SEN,L}$ [mm]	f_{SEN} *(friction factor)*	f_L , L [mm]	f_A , A [mm^2]	**Flow rate** Q [m^3/s]
Run 4	49.1	0.049	1.000, [49.1]	1.000, [1893]	0.0057
Run 5	58	0.047	0.612, [35.5]	0.519, [1370]	0.0057
Run 6	75	0.042	0.415, [31.1]	0.300, [1325]	0.0057
Run 7	100	0.038	0.278, [27.8]	0.168, [1323]	0.0057

(All other casting conditions are same to the previous slide table)

Fig 17. Relations between the slide-gate opening fraction f_L and the flow rate Q depending on the SEN &UTN diameter

Parametric study 2 results: Nozzle diameter ($D_{SEN} = D_{lower} = D_{slide} = D_{UTN}$)

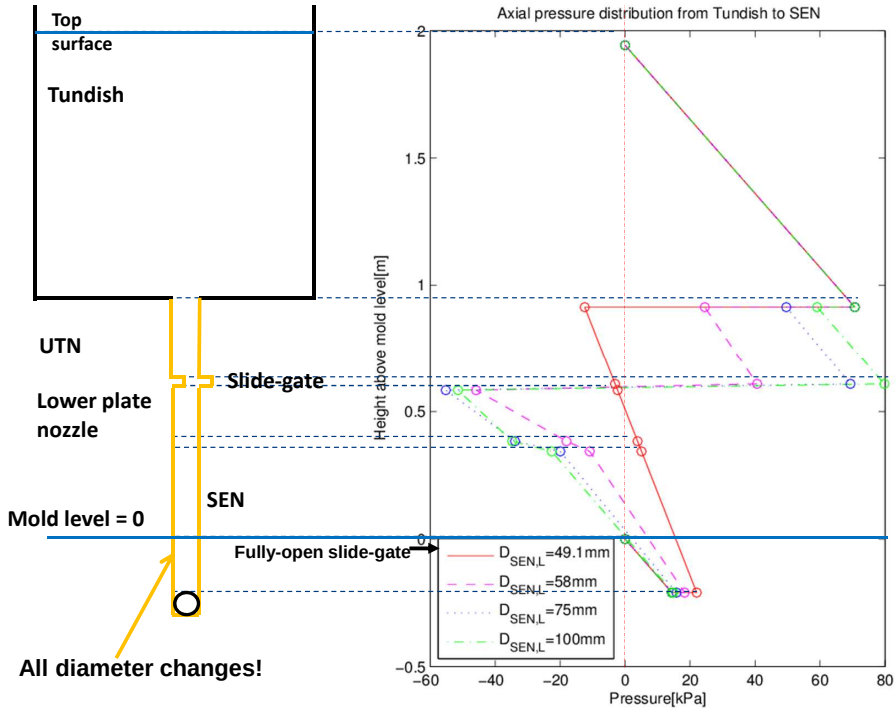

- Even with fully-open slide-gate (49mm), some negative pressure arises at both tundish bottom and at slide-gate.

Fig 18. Axial pressure distributions depending on the different SEN diameters

Mechanism

- Avoiding air aspiration due to negative pressure at the slide-gate joints requires a redistribution of the pressure drop to consume the potential energy generated by the height difference.
- Thus: increasing pressure drop below the slide-gate (by decreasing lower nozzle and SEN diameter) is advantageous due to:
  - Increased friction loss (both straight sections and "minor loss" transition regions)
  - Increased velocity (requiring converting more potential energy into kinetic energy)
- Tapering ($D_{UTN} > D_{SEN}$) is beneficial because it increases the portion of pressure drop occurring below the slide-gate.

$\Sigma\rho e_{Labove} \propto V_{UTN}^2 \propto 1/D_{UTN}^4$ — Losses **above** the slide-gate

$\Sigma\rho e_{Lbewlow} \propto V_{SEN}^2 \propto 1/D_{SEN,D}^4$ — Losses **below** the slide-gate

$$\underbrace{\rho g(H_{TUN} + h_2)}_{\text{Potential E (input)}} = \underbrace{\frac{1}{2}\rho V_{port}^2}_{\text{Kinetic E (output)}} + \underbrace{\rho e_{Ltun} + \Delta P_{two} + \rho e_{Lslide}}_{\text{Losses above}} + \underbrace{\rho e_{Lcont} + \rho e_{Lport} + \rho e_{Ltee} + \rho e_{Lf}}_{\text{Losses below}}$$

$\Sigma\rho e_L$: energy losses in the system

Conclusions

- A 1D analytical model is developed for pressure distribution in the CC flow delivery system (from the tundish top surface to the mold top surface).
- Pressure distribution is validated by roughly matching both a 3D numerical simulation and several plant measurements.
- Smaller SEN diameter is beneficial to decrease negative pressure.
  - Smaller SEN diameter requires a larger slide-gate opening -> less pressure drop through the slide-gate
- Apply model to typical commercial caster suggests:
  - Current SEN diameter of 75mm causes negative pressure below slide gate
  - Decreasing SEN diameter to 50mm or less (keeping other nozzle dimensions constant) should avoid negative pressure
  - Gate opening increases from 38% (75mm $D_{SEN,L}$) to 45% (52mm $D_{SEN,L}$) to maintain casting speed
- Decreasing all diameters together (UTN, upper plate, slide gate opening, lower plate, lower nozzle, and SEN) is not recommended because
  - 1) negative pressure still arises and
  - 2) this requires large increase in gate opening, which makes the system more vulnerable to clogging.

Acknowledgments

- Continuous Casting Consortium Members (ABB, AK Steel, ArcelorMittal, Baosteel, JFE Steel Corp., Magnesita Refractories, Nippon Steel and Sumitomo Metal Corp., Nucor Steel, Postech/ Posco, SSAB, ANSYS/ Fluent)

- Special thanks to Xiaoming Ruan for the plant data from Baosteel.

References

1. Bai, H. and B. G. Thomas, “Effects of Clogging, Argon Injection, and Continuous Casting Conditions on Flow and Air Aspiration in Submerged Entry Nozzles,” Metallurgical and Materials Transactions B, 32B:4, 707-722, 2001

2. Liu Rui, Brian G. Thomas, Bruce Forman and Hongbin Yin, "Transient Turbulent Flow Simulation with Water Model Validation and Application to Slide Gate Dithering," AISTech 2012, (Atlanta, GA, May 7-9, 2012), 2012

3. Han et al., “Sliding gate assembly and method for controlling the same”, KR20120026720

4. B.G. Thomas ME550 (solidification) lecture note (2015)

5. L. F. Moody, “Friction factor for pipe flow,” transactions of the ASME (1944)

6. White, *Fluid Mechanics* 7th Edition (2011)

7. Armaly, B. F., F. Durst, J. C. F. Pereira, and B. Schönung. “Experimental and Theoretical Investigation of Backward-Facing Step Flow.” *Journal of Fluid Mechanics* 127, no. -1 (February 1983): 473.